Economies of Complexity of 3D Printed Sand Molds for Casting

Ashley Martof[1], Ram Gullapalli[2], Jon Kelly[3], Allison Rea[3], Brandon Lamoncha[4], Jason M. Walker[3], Brett Conner[3], Eric MacDonald[3]

[1] Youngstown Business Incubator, Youngstown, OH 44555
[2] Case Western Reserve University, Cleveland, OH 44106
[3] Advanced Manufacturing Research Center, Youngstown State University, OH 44555
[4] Humtown Products, Columbiana, OH 44408

Abstract: Additive Manufacturing (more commonly referred to as 3D printing) is resulting in a metamorphosis of the sand casting industry as 3D printed sand molds enable castings of unmatched geometric complexity. The manifold benefits of these molds include: (1) the integration of structural elements such as periodic lattices in order to optimize weight versus strength; (2) the structural inclusion of unique features such as embossed part numbers and/or other details of the production history; and (3) complex geometries that generate new casting applications not possible previously. Additive Manufacturing is often described as providing "complexity for free", which may not be entirely precise but generally holds true and the identification of castings that are sufficiently complex to benefit from 3D printing is generally left to the intuition of the designer or foundry. New software tools are necessary for foundries to discover opportunities in which the additional costs of 3D printing are compensated by the benefits of increased structural complexity. This paper describes a complexity evaluation tool that scores CAD models to determine the most economical casting approach based on slicing and 2D geometry evaluation. The three potential outcomes include (1) traditional sand casting, (2) AM-enabled sand casting and (3) a hybrid of the two with 3D printed cores in traditional casting flasks. Several case studies are described and evaluated.

1.0 Introduction

Sand casting is an economical metal process that was used as early as the Shang Dynasty of China in 1,000 BC (Barnard 1961). In comparison to other forms of casting, sand casting provides a wide range of casting sizes, complexity, and processable metals. Consequently, the size of the global market recently exceeded 100 million metric tons (Staff 2016) with sand as the predominant method of casting (USITC 2005). The significance of this ancient industry requires the leveraging of the latest simulation and analysis tools to identify opportunities for 3D printing of both sand molds and cores.

Additive manufacturing was invented in the 1980s and was generally relegated to creating form and fit prototypes; however, the possibility of leveraging 3D printing for casting was recognized as soon as a decade later (Hull et al. 1995; Cheah et al. 2004). The ability to fabricate

geometrically complex parts using layerwise deposition as opposed to traditional subtractive manufacturing now allows for molds and cores that would be otherwise impossible without 3D printing (Bassoli et al. 2007). Important benefits of 3D printed sand molds are complex cavities, tight dimensional accuracies, components insertion within the casting and/or mold (ceramics or other metal structures), and an increased freedom in the design of the molten metal delivery system (gating and risers). At least initially, 3D printed sand molds and cores also provide improved delivery times as hard tooling is not required and all molds are rendered from computer designed files in software. Consequently, 3D printed sand molds have lead to an immediate impact on low volume and bridge production as well as design and prototype iteration.

Understanding the decision boundary between when a casting is more suitable for traditional methods versus 3D printing is important in order to close the business case. Furthermore, some scenarios are best suited for a hybrid approaches which allow for complex internal cavities to be formed with 3D printing while the outer features are created using traditional cope and drag casting methodology. Fig. 1 left shows a casting that could not be fabricated with traditional casting while the right figure shows a traditional casting using a pattern and core.

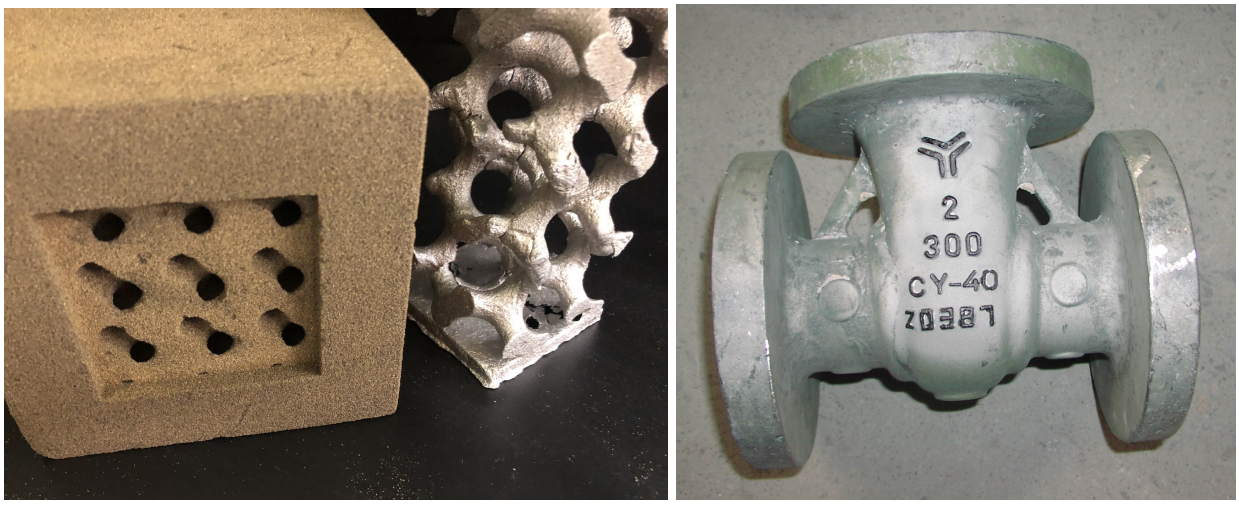

Figure 1: Complex casting with 3D printed mold (left) and traditional casting with traditional cores and molds (right - courtesy of wikicommons)

As a result of the potential benefits, many groups have explored evaluating geometrical complexity in the context of 3D printing for casting in which different challenges were addressed or the benefits of 3D printing were identified (Atzeni and Salmi 2012; Upadhyay, Sivarupan, and El Mansori 2017; Hackney and Wooldridge 2017; Deng et al. 2018; Shangguan et al. 2017; Snelling et al. 2013; J. Walker et al. 2018; Mun et al. 2015; Singh 2010). Research has been conducted on the economics of conventional manufacturing versus additive manufacturing of end usable part production (Atzeni and Salmi 2012; Manogharan, Wysk, and Harrysson 2016;

Hopkinson and Dicknes 2003; Baumers et al. 2016/1; Almaghariz et al. 2016; Conner et al. 2014; Martof and Conner 2017); (Thomas and Gilbert 2014), research has concluded parts with high complexity and/or low volume result in cost savings when utilizing additive for part production. Research on part shape complexity and the effect complexity has on energy consumption in additive manufacturing has also been looked into (Baumers 2012; Psarra and Grajewski 2001). However, fewer groups have investigated evaluating the complexity of the structure directly in order to inform the economic decisions of using 3D printing for casting (Almaghariz et al. 2016; Conner et al. 2014; Martof and Conner 2017). Research has been conducted on the complexity of castings calculated using a regression analysis based on parameters from a CAD model (Almaghariz et al. 2016; Joshi and Ravi 2010). Part volume ratio, area ratio, number of cores and core volume ratio are a few of the parameters used to calculate the shape complexity. This complexity factor formula was further researched in (Gullapalli 2016) and used to calculate cost of different manufacturing processes. Four different scenarios related to sand casting were considered. Traditional manufacturing of sand casting, 3D sand printing of molds and cores, 3d sand printed cores with traditional molds, and 3d printed patterns. Two cases studies were used to study the relationship between complexity to manufacturing costs and determine the economical manufacturing method. This previous work, case studies and complexity factor serve as a basis for the algorithms developed in this paper.

2.0 Materials and Methods

2.1 Complexity Algorithm

Complexity can be calculated with many geometrical methodologies in order to identify the complex features that are relevant to castings, and more specifically, features that require 3D printing (e.g. overhangs, internal voids requiring cores, low draft, ribs, parting line avoidance, cross section uniformity, etc.). These pathological features requiring the use of 3D printing are being indirectly measured in this work by slicing an STL of a final part into layers and then performing analysis on each 2D slice by interrogating detected contours. In this study, four algorithms were identified and were inspired from the works of others (Joshi and Ravi 2010; Almaghariz et al. 2016; Gullapalli 2016; Baumers 2012; Watson 2011); (Psarra and Grajewski 2001) and based on the intuition of the authors. For each layer, two complexity numbers were calculated for each algorithm in order to simultaneously evaluate the exterior and interior complexity. Interior complexity is posited to provide data about the need for 3D printed cores, while the exterior complexity informs the decision about whether a flask is required to be 3D printed or if traditional techniques are more suitable.

Four algorithms were developed that all began by slicing each of the benchmark STL files and performing analysis per layer producing an average complexity across all layers. This process was repeated for three orientations of each part and the results were averaged including: an unrotated case, a rotated case 90 degrees in X axis and rotated 90 degrees in Y axis. The

rotations were completed in order to detect a complexity bias relative to orientation. For each orientation, the complexity numbers from all layers were individually calculated and then the total was divided by the number of layers for a mean value that was independent of the number of slices selected. By using more layers, the accuracy was expected to improve by improving the statistical sampling; however each additional layer meant an increase in the duration of computation. For this study, 10 layers were used and each layer image was confined to 1000 rows and 1000 columns - all three numbers of which directly impact the computation duration.

Each algorithm leveraged existing analysis features of the Python libraries - OpenCV and Numpy-STL - for finding contours, calculating perimeter length and area and identifying concavity and convexity features of the contour. OpenCV is open source and when coupled with the libraries Numpy and Matplotlib with Python as a language, provides a framework similar to Matlab and is well suited for efficiently reading STL files and performing a rich set of geometry functions to extract features and evaluate complexity.

Algorithm A: Number of contours per layer

The first algorithm was the simplest and just summed the number of contours detected for each layer. Contours that were parents in the hierarchy (exterior contours) were added to the exterior complexity number, and conversely, the child hierarchy elements were counted separately as the interior. Both values were reported to help to identify the correct casting methodology. Fig. 2 shows algorithm A in action with the STL rendered and two layers illustrated.

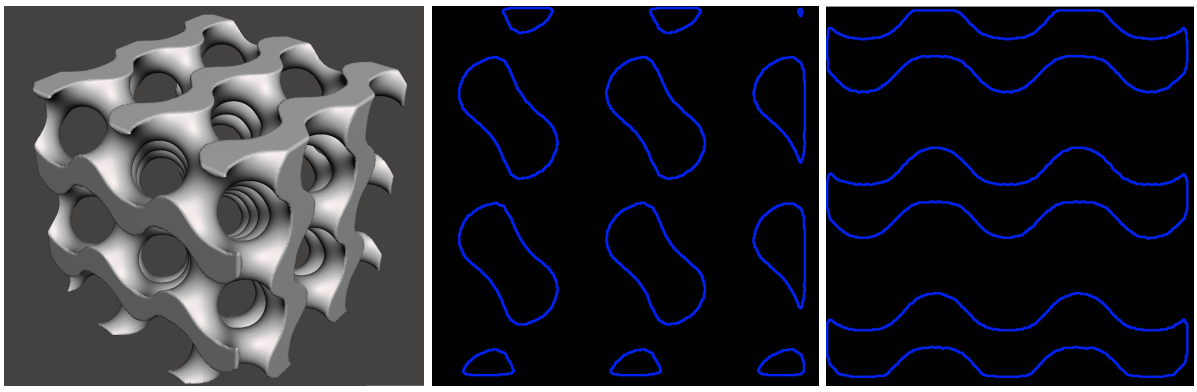

Figure 2: Example of two layers in which contours are summed per layer. The STL of a gyroid matrix (left), one layer with nine contours and a score of nine (center) and another example layer with three contours and score of three (right).

Algorithm B: Ratio of contour perimeter to contour area per layer

Algorithm B is similar to A except that instead of incrementing the sum of contours, a ratio was calculated and added to a running sum. This algorithm is similar to research conducted by NASA

on perimetric complexity of binary images (Watson 2011). The ratio captured included the length of the perimeter of a given contour divided by the area of the contour. A circle would provide intuitively the smallest ratio and is therefore considered "simple". An alternative and more complex shape like a star would have a larger perimeter while maintaining a similar area and the increased ratio would emphasize that the shape was more complex than the circle. All ratios per layer were summed and all layers were averaged.

Algorithm C: Number of concave features per contour per layer

This algorithm summed the number of contours but also included a sum of concavity defects that were sufficiently concave. A convex hull is the contour that encloses a contour in question but without any concave features - the same contour if no concavity exists or a larger contour circumscribing the original. Any point at which the two contours diverge with the greatest separation is defined as a concavity defect and several are shown as red dots in fig. 3 for two different layers of a dragon STL. This algorithm provides a score that is directly proportional to the number of contours plus the number of concavity defects for all contours on a given layer. Intuitively, concavity defects are an indication that the structure is complex in the context of the casting as these features can interfere with the use of patterns in traditional casting.

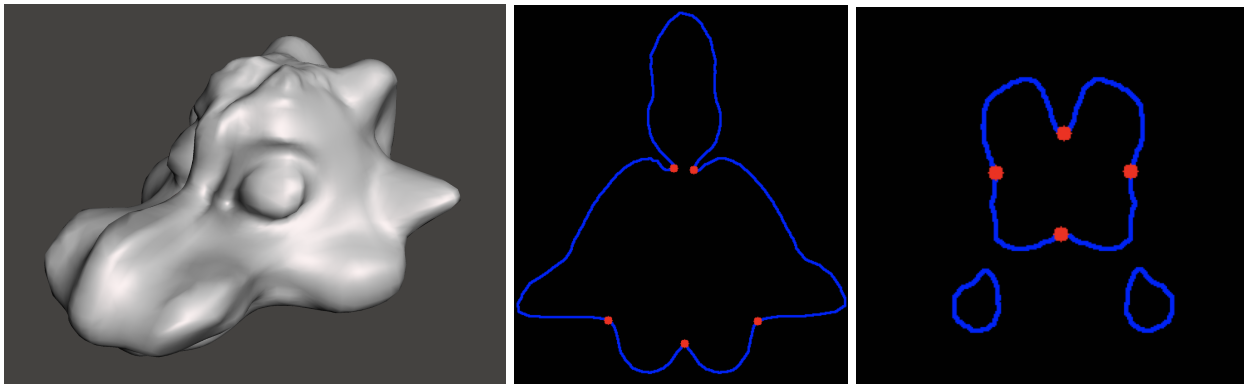

Figure 3: Example of two layers in which contours and concavity defects are summed. The STL (left), one layer with five concavity defects, one contour and a score of six (center) and another example layer with three contours and four concavity defects and score of seven (right)

Aggregate Algorithm (D): "All of the Above"

This algorithm was an aggregate of the other algorithms: the contours, the ratio of perimeter over area and the number of concavity defects summed together. The aggregate algorithm is the most comprehensive measurement - capturing the number of contours, the complexity and concavity of each contour. This consensus approach provided manifold perspectives in order to identify cases that may be pathological in terms of determining if a casting requires 3D printing and was identified as the most effective.

2.2 Benchmark Casting Families

Sixteen structures intended for casting were selected. The first two were very simple geometries: a solid sphere and a sphere containing a spherical cavity in order to evaluate the lower bound of complexity from both the internal and external perspectives. In order to provide examples in the upper bound of complexity, a Voronoi tessellation chess piece and a gyroid matrix were selected (fig. 4 left). The queen chess piece was designed using voronoi tessellation. The Schoen's gyroid (fig. 4. left center) falls into a class of mathematical surfaces referred to as triply periodic minimal surfaces (TPMS) which separate 3D space into two complex and intertwined but separate phases . Here, one phase is established as a solid network of struts, while the second phase is void and constitutes the porous volume. Due to their mathematical complexion, TPMS-derived structures are extremely manipulable and computationally efficient; however they are difficult if not impossible to cast with traditional methodologies. From a metal casting standpoint, both the chess piece and gyroid part would require 3D printed tooling to cast.

Two additional industrially-relevant castings were included as both models were used in a previous economic and complexity study, the results of which are used as a baseline in this study with computer vision libraries. Both castings are provided by Humtown Products with one case including an air brake (fig 4. center right). The design package consists of one mold design and eight core designs. For this research, a family of castings was created with increasing levels of complexity by incrementally increasing the number of cores while maintaining the outer mold line dimensions. Hence a total of eight sub-cases were created by beginning with the first sub-case (a solid casting with one mold and no cores) and then incrementally adding one extra core. It should be noted that for the complete design, conventional manufacturing involves fabricating eight hard core boxes to make eight cores which leads to issues with damage during transportation, breakage during assembly, misassembly, core shift, and flash at core bonding points. With 3D sand printing, the eight cores become consolidated to a single core.

The second previously studied casting was a turbocharger also provided by Humtown Products. This consists of a mold and core design (fig. 4 right) and the complexity was changed by varying the number of cores. Hence four sub-cases were created, where each sub-case has an additional core and the four cases are: (1) solid turbocharger, no interior cavity and no cores, (2) a single cube shaped cavity (one core), (3) two cylindrical shaped cavities (two cores), and (4) the original design (requiring three traditionally manufactured cores which can be consolidated to one core using 3D sand printing).

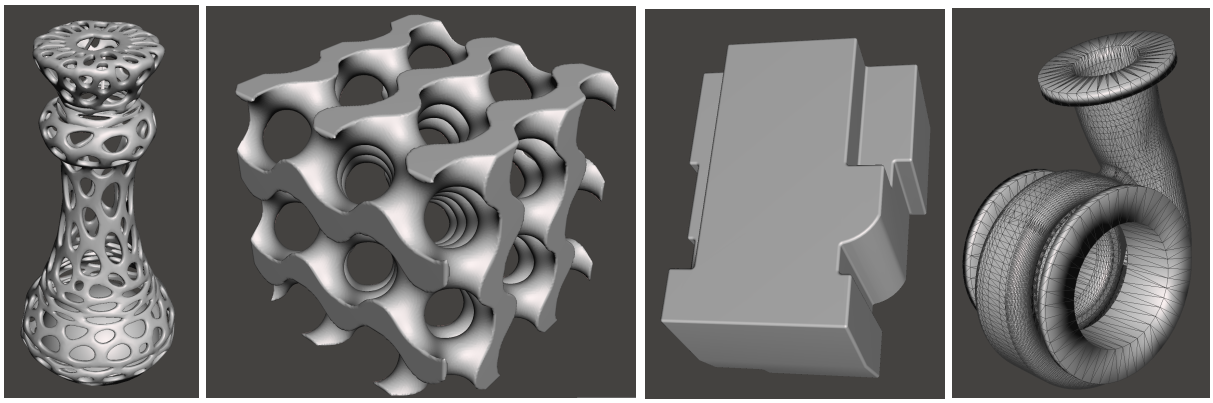

Figure 4: Montage of the benchmark structures used in this analysis: (left) voronoi chess piece, (left center) gyroid matrix, (right center) air brake, (right) turbocharger.

3.0 Results and Discussion

The different castings were run through the complexity software and the results are in Table 1 which summarizes the scores of the four complexity algorithms on the sixteen test structures. These data are then compared to complexity scores assigned by previous work in which the scores were generated manually and correlated well with the decision as to which casting process was most suitable. One major difference with the software automated approach described in this paper is that the original work did not capture internal versus external complexity. To compare the current work to the previous study, a composite score was generated and this was in good agreement with the original work (monotonically related).

3.1 Software Complexity Evaluation

Selected to demonstrate the lower bound of complexity, the Solid Sphere and Sphere with Cavity both have relatively low exterior complexity valuations, as would be expected. Furthermore, the Solid Sphere has 0.000 or null interior complexity as there are no interior features. Meanwhile, the Sphere with Cavity has low but existent interior complexity corresponding to its simple spherical cavity. In all cases (except null), the complexity value increases from Algorithm A to Algorithm D, as more features are included in the computation and the difference between the two sphere exteriors is primarily driven by resolution and rounding error. Fig. 5 displays the complexity factor values for each of the benchmark castings as computed by each of the four algorithms for both interior and exterior features.

The Air Brake and Turbocharger families further illuminate the ability of the algorithms to discriminate complexity as it relates to selecting a casting technology.. In the Air Brake family, all of the designs have the same external geometry and have increasingly more complicated internal geometries from Design One to Design Eight. The identical exterior complexity of all eight Air Brakes is captured well with all of the exterior complexity scores. The only minor

differences are calculated and these can be attributed to slightly different geometric boundaries where different internal features interface with the external surface and modified the outer form slightly. Air Brake - 1 (AB1), the simplest of all, was determined to have a exterior complexity (for the rest of this paper, all complexity scores are based on the D Algorithm) of 3.128 while AB8, the most complex of all, was determined to have a similar exterior complexity of 2.953. However, while AB1 only had an internal complexity of 1.556, each subsequent Air Brake design had increasing internal complexity culminating in an internal complexity for AB8 of 6.187 - nearly four times higher. A similar trend is seen with the Turbocharger family. These complexity scores, therefore, provide a very efficient method to differentiate between complexity of structures, even when they may appear to be very geometrically similar from the exterior.

The Voronoi Chess Piece and Gyroid Matrix are immensely different but provide very clear complexity scores. By visual analysis alone, it is obvious that both benchmark structures have high exterior complexity and the scores capture this. With exterior complexity scores of 17.082 (Voronoi) and 27.580 (Gyroid), the two structures are rated as orders of magnitude more complex with respect to their exterior surfaces than all of the other benchmark castings. Interestingly, both of these structures have extremely low or null interior complexity scores. This is a function of the character of lattice structures. Because all of the interior space is interconnected, little or none of it is discriminated as actually internal. In cases like these, however, the internal score is irrelevant though as the external score is high enough to indicate the necessity for the entire mold package to be 3D printed.

Furthermore, differentiating between external and internal complexity is paramount to selecting the most efficient manufacturing method for mold production. Low external complexity generally indicates that a traditional sand mold can be effectively used with hard tooling, whereas high external complexity would likely indicate the need for a complete 3D printed mold package (i.e. The Voronoi Chess Piece and Gyroid Matrix). In the case of low external complexity, though, there are still cases of low and high internal complexity. Low complexity scores for both internal and external may be indicative of a case for entirely traditional methods of mold production - that is, cases requiring simple cores or no cores at all. Conversely, the case of low external complexity and high internal complexity would indicate that traditional molding may be used for the cope and drag but additive manufacturing would be effective to address the need for intricate cores.

Table 1: Complexity results for the benchmark structures.

Algorithm	Exterior Complexity				Interior Complexity			
	AE	BE	CE	DE	AI	BI	CI	DI
Solid Sphere	1.000	1.011	1.000	1.011	0.000	0.000	0.000	0.000
Sphere wih Cavity	1.370	1.868	1.666	2.164	0.888	0.896	0.888	0.896
Voronoi Chess Piece	10.037	12.045	15.074	17.082	0.111	0.113	0.518	0.521
Gyroid Matrix	14.074	22.062	19.592	27.580	0.000	0.000	0.000	0.000
Air Brake - 1	1.259	1.387	3.000	3.128	0.851	0.889	1.518	1.556
Air Brake - 2	1.333	1.479	3.111	3.256	1.111	1.139	2.296	2.324
Air Brake - 3	1.333	1.464	3.148	3.279	1.259	1.291	2.259	2.291
Air Brake - 4	1.333	1.460	3.259	3.390	1.592	1.641	2.851	2.901
Air Brake - 5	1.333	1.464	3.259	3.390	1.814	1.878	3.296	3.359
Air Brake - 6	1.370	1.503	3.333	3.466	2.222	2.804	4.296	4.378
Air Brake - 7	1.407	1.541	3.407	3.541	2.666	2.766	5.259	5.359
Air Brake - 8	1.259	1.398	2.814	2.953	3.000	3.112	6.074	6.187
Turbocharger - 1	2.000	2.150	5.962	6.113	0.000	0.000	0.000	0.000
Turbocharger - 2	2.074	2.156	5.592	5.675	0.074	0.075	0.074	0.075
Turbocharger - 3	2.222	2.394	6.337	6.542	0.185	0.203	0.185	0.203
Turbocharger - 4	2.259	2.467	7.259	7.467	0.703	0.759	1.444	1.500

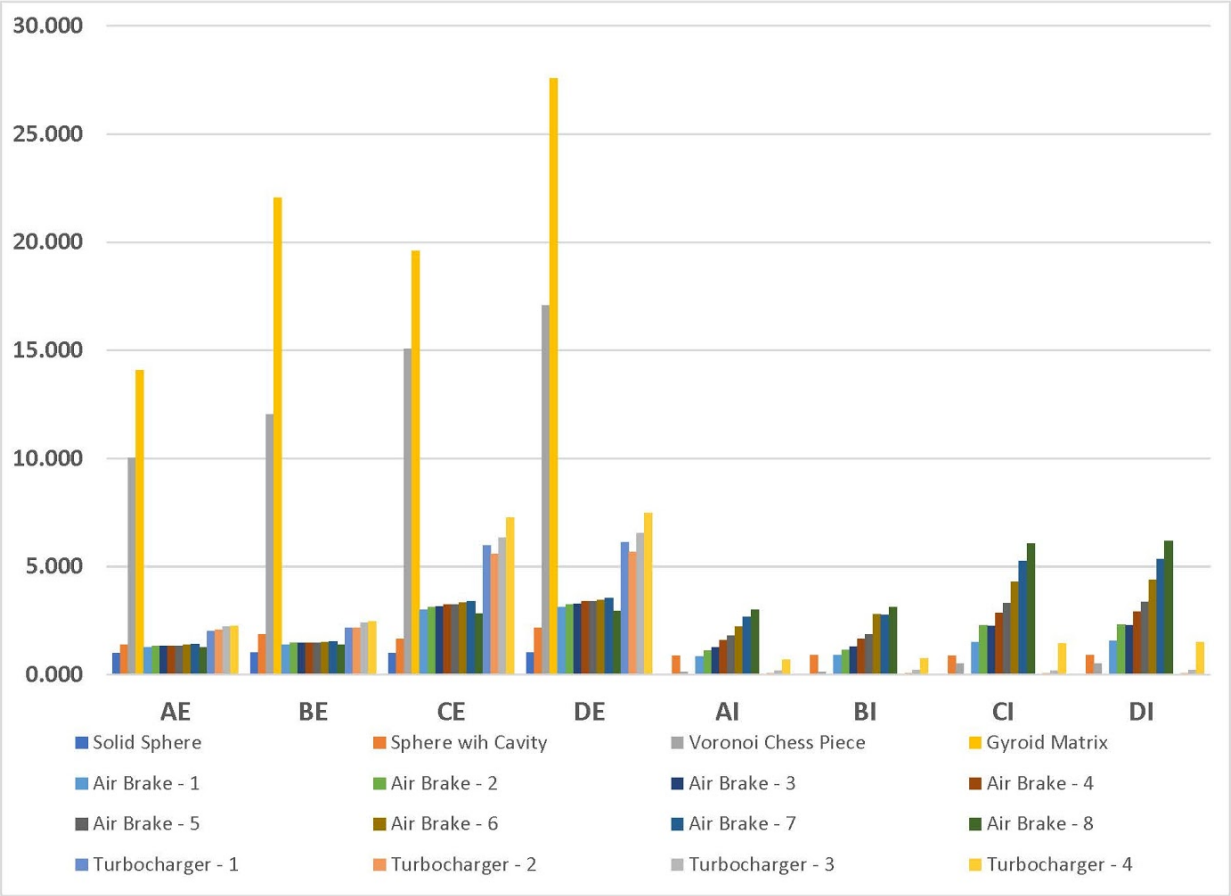

Figure 5: The complexity factor values for Algorithms A-D are shown for each of the benchmark castings. E indicates exterior. I indicates interior.

3.2 Comparison to Previous Studies

Previous complexity factor analysis of the air brake family was completed in (Almaghariz et al. 2016) using a complexity factor model designed for castings developed by Joshi and Ravi (Joshi and Ravi 2010). The J&R model requires knowledge of casting design by requiring (among many factors) inputs for the number of cores required and the volume of those cores. A goal of this layerwise complexity factor shown in this paper is to eliminate that design knowledge constraint. Figure 6 shows each of the eight layerwise complexity factors plotted against the J&R model complexity factor for the air brake family of castings. It should be noted that the J&R model considers the casting as a whole and thus includes the exterior and interior complexity together without separation. Consequently, exterior complexity factors (AE through DE) are nearly constant compared to J&R model values.

A more constructive approach would be examining the summation of exterior and interior complexities. Here we choose the summation of Algorithm D's exterior complexity (DE) and

interior complexity (DI). This is now plotted against the J&R model complexity factor in fig. 7. The turbocharger family of castings are included in this graph. The trends are now very similar between the two models but the results are different for the two families. A common reference would be desirable. Weighting the layerwise complexity factors is an option.

By inspection, one can choose weights and obtain the following relationship (eq. 1):

$$Weighted\ Layerwise\ Complexity\ Factor\ (WLCF) = 0.75\,DE + 12.5\,DI \qquad \text{eq. 1}$$

This is now plotted in fig. 8. Here the air brake and turbocharger values lie nearly on top of each other and agree well. In fact, the following polynomial function (eq. 2) can be plotted through the points with a R^2 of 0.9679.

$$WLCF = 6 \times 10^{-6} JRCF^4 - 9 \times 10^{-4} JRCF^3 + 0.0485 \times JRCF^2 - 1.2292 \times JRCF + 16.243 \qquad \text{eq. 2}$$

Consequently, the Weighted Layerwise Complexity Factor is a viable method for geometric complexity analysis that does not require detailed knowledge of conventional/traditional fabrication processes.

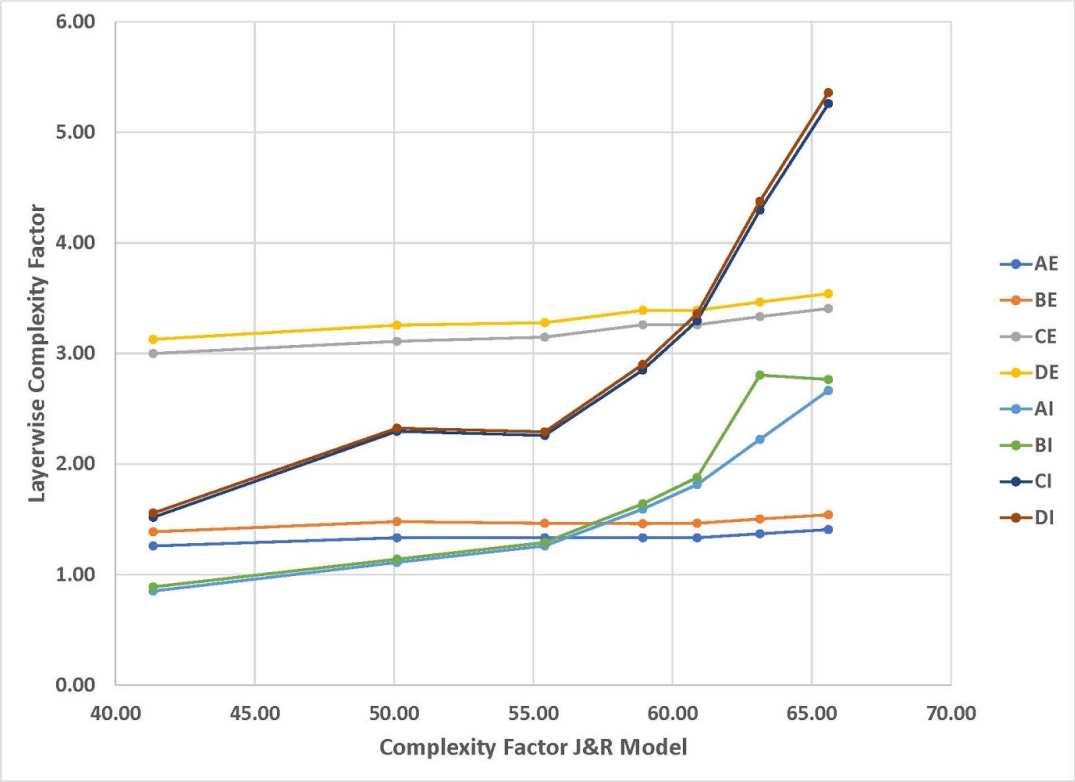

Figure 6: Each of the eight layerwise complexity factor values are plotted against the values calculated in (Almaghariz et al. 2016) for the J&R model.

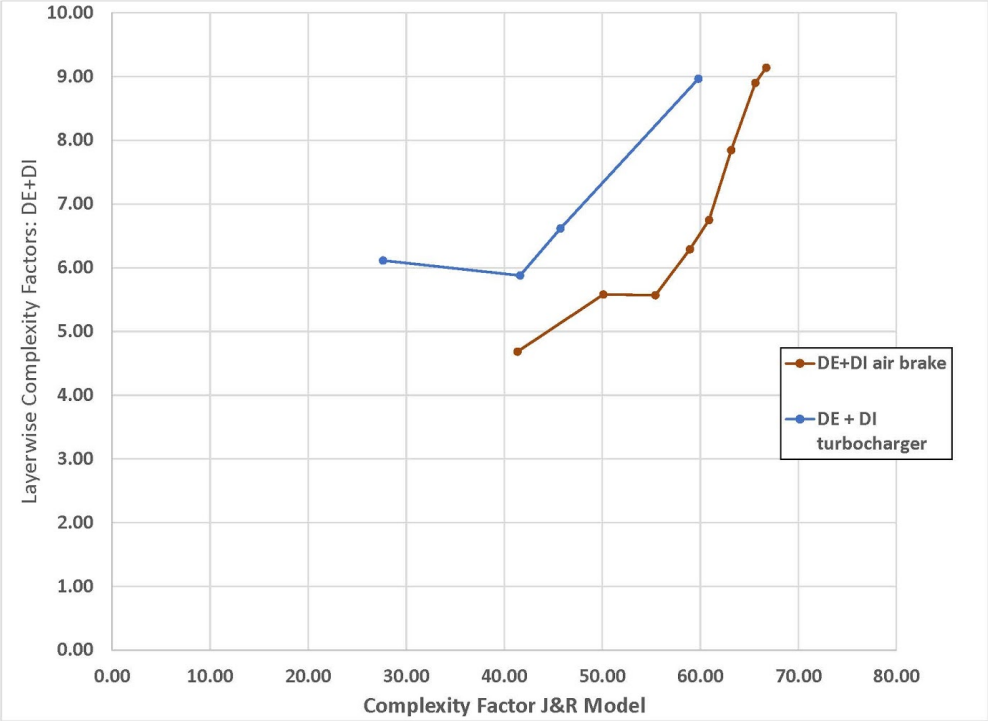

Figure 7: The exterior (DE) and interior complexity (DI) of Algorithm D are added together and plotted against the J&R model complexity factor.

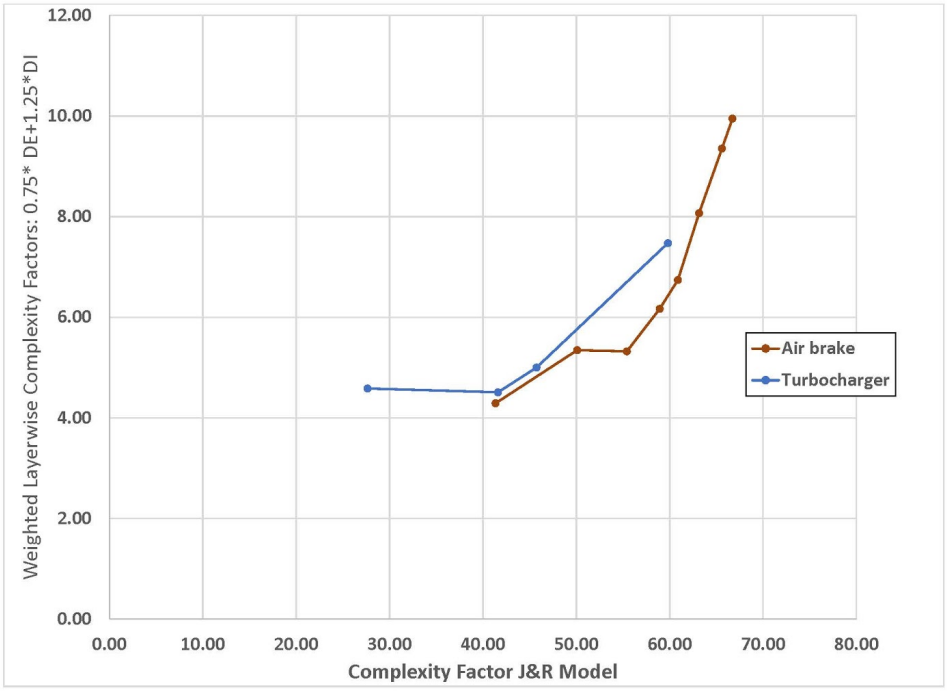

Figure 8: A weighted layerwise complexity factor is plotted against the J&R model

For an economic analysis, we will consider four different methods of fabrication:

- Traditional manufacturing (TM): Traditional subtractive processes to make molds / cores.
- 3D Sand Printing (3DSP): Complete sand printing of both molds and cores.
- 3D Sand Printed Core (3DSPC): 3D sand printing of cores and conventional pattern making for the mold - cope and drag.
- FDM Pattern-making (FDMP): Conventional core making and 3D printing using fused deposition modeling of hard patterns for conventional mold making with the advantage of faster mold fabrication.

The cost model elements for each can be found in (Gullapalli 2016). Here we consider application of complexity factors and cost modeling to the economics of mold and core sets for the air brake family of castings. Figures 9, 10, and 11 are three graphs plotting cost per part as a function of complexity (using the weighted layerwise complexity factor from above) for three different production quantities: 1, 100, 1000. The process with the lowest cost per part is the most economical for a given value complexity. The most economical process will vary as a function of complexity and quantity. For example, in Figure 9, the most economical process is 3DSP regardless of level of complexity. However, at quantities of 100 as shown in Figure 10, then for castings with complexity of 5 or higher, 3DSPC is the most cost effective method of mold and core sets. For castings of low complexity, then FDMP is the cost effective. For quantities of 1,000 as shown in Figure 11 then 3DSPC becomes the most cost effective for the full range of complexities for this family of castings. The value of the complexity factor is to help choose the most cost effective method of production.

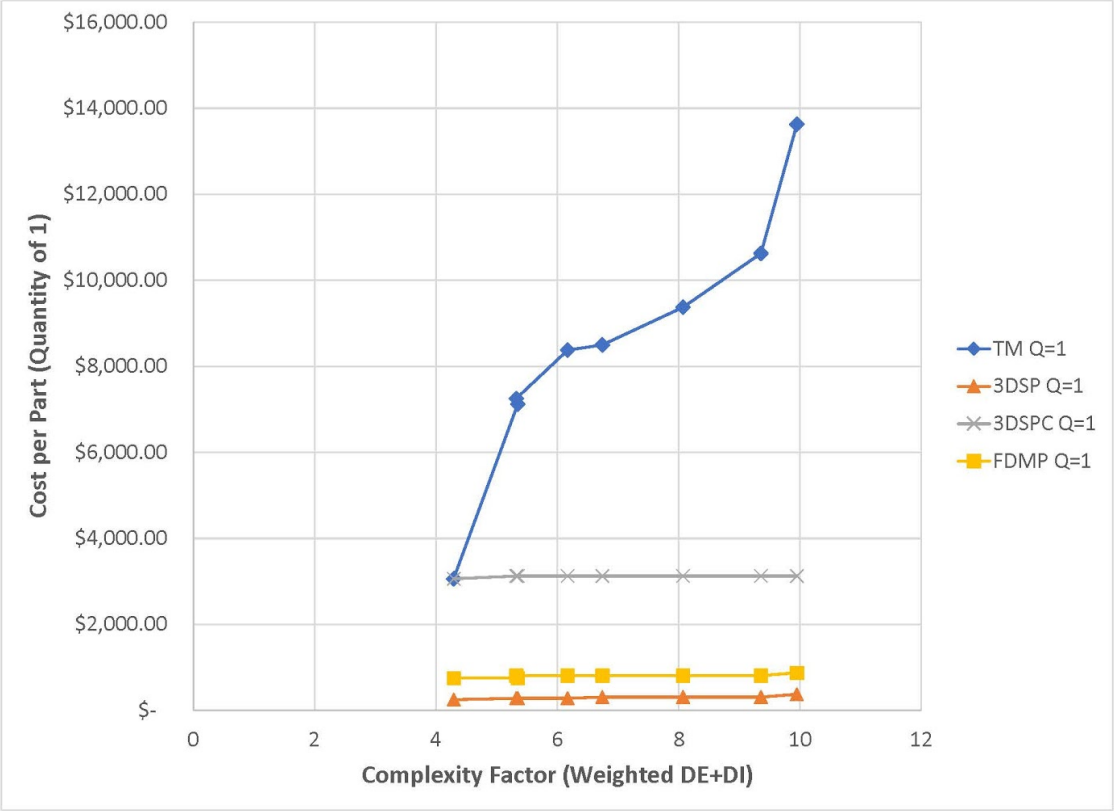

Figure 9. Mold and core set cost versus complexity of air brake family of parts for quantity of one.

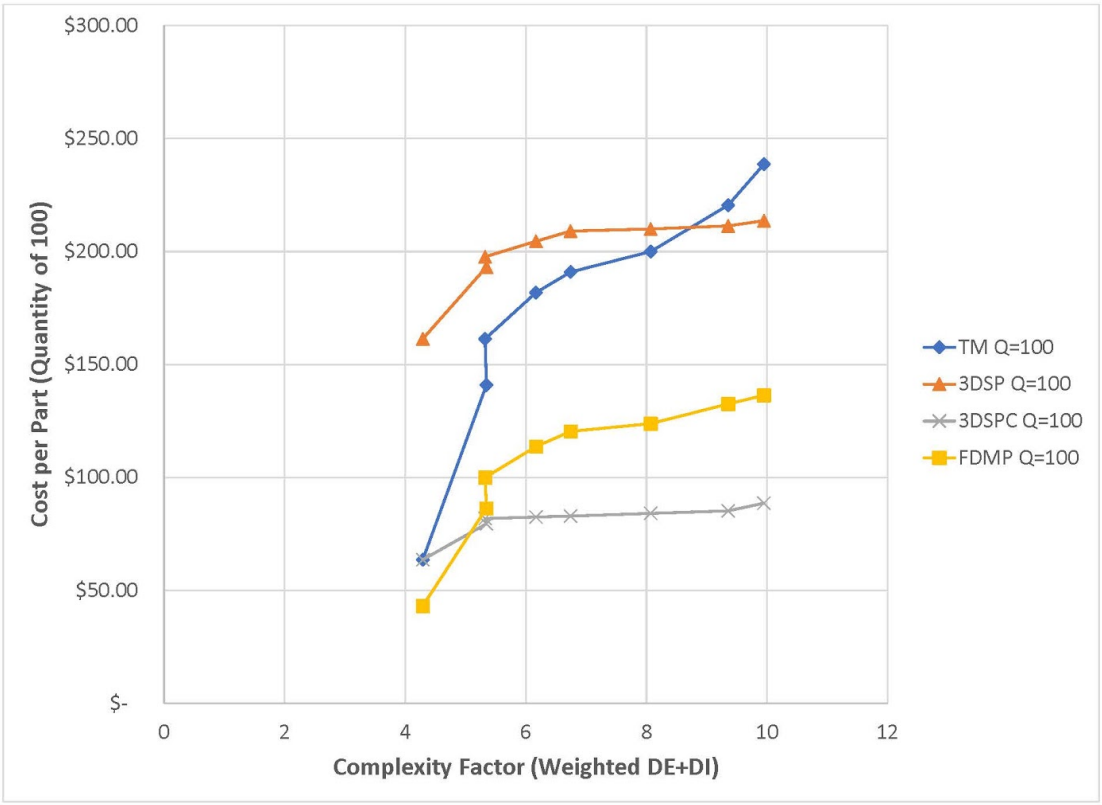

Figure 10. Mold and core set cost versus complexity of air brake family of parts for quantity of one hundred.

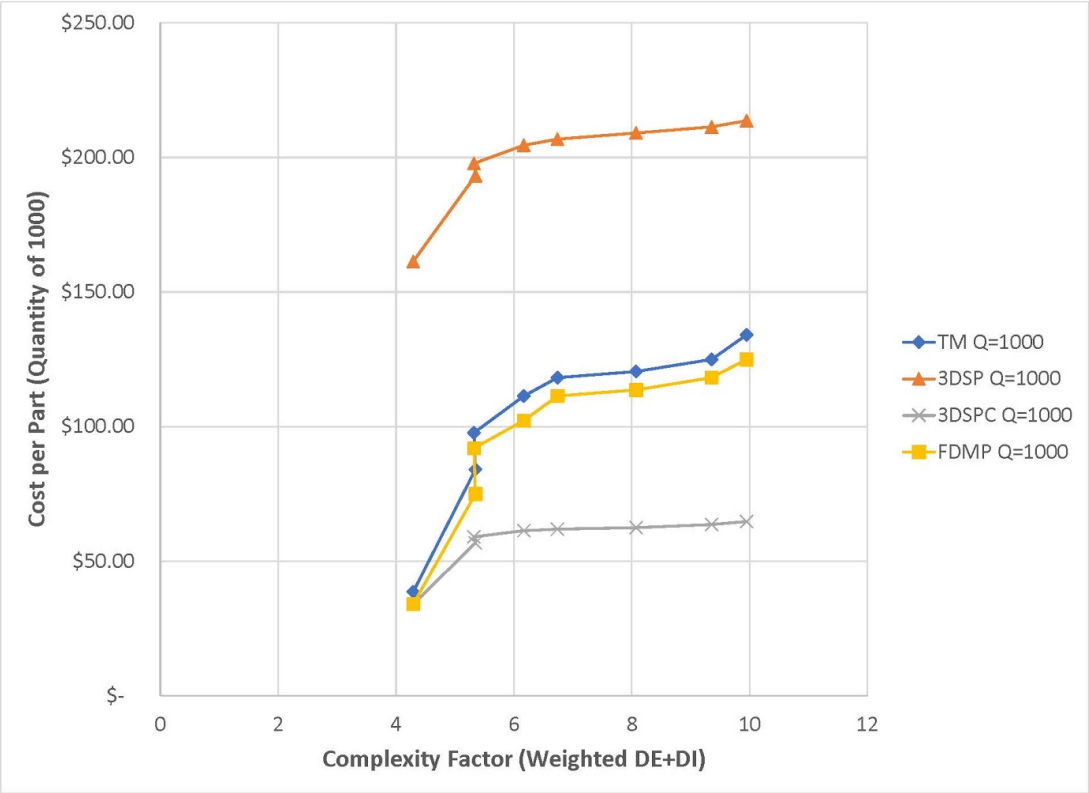

Figure 11. Mold and core set cost versus complexity of air brake family of parts for quantity of 1,000.

Future work may include the addition of a three dimensional complexity analysis of STL part files. In a previous work, a methodology was developed to calculate 3D signed distance fields of STL files and to subsequently reconstruct 2D and 3D contours based on a level set approach (J. M. Walker et al. 2017). The signed distance field generator is agnostic to the input shape and contains a large amount of geometric and topological data including defining internal and external space, distances to all faces, edges, and vertices, and normal vectors of all faces, edges, and vertices. Combined with the layerwise analysis of contours, a supplementary three dimensional analysis score could further elucidate complexity.

4.0 Conclusions

3D printing stands to transform the casting industry - particularly in cases of low volume, bridge production, customized or complex castings. In order to inform the business decision as to whether 3D printing makes sense - either fully or hybrid (only cores are printed), this research demonstrated a relatively simple 2D slicing approach for measuring complexity of the casting geometries. The finding show that of the four algorithms, the “all of the above” gave values that provide a decision boundary that was in line with the intuition of the authors as well as obvious extreme cases (sphere as a case of simplicity or a gyroid matrix for a case that can only be cast

with the help of 3D printing). This layerwise complexity factor was compared to a known complexity factor for conventional casting fabrication method and showed similar results but without requiring design knowledge of the traditional methods. The economics of complexity and quantity were shown for a traditional casting tooling method and then compared to three methods that involved additive manufacturing.

Acknowledgements

We would like to thank the Friedman Endowment for Manufacturing at Youngstown State University for supporting this project.

References

Almaghariz, Eyad S., Brett P. Conner, Lukas Lenner, Ram Gullapalli, Guha P. Manogharan, Brandon Lamoncha, and Maureen Fang. 2016. "Quantifying the Role of Part Design Complexity in Using 3D Sand Printing for Molds and Cores." *International Journal of Metalcasting* 10 (3): 240–52.

Atzeni, E., and A. Salmi. 2012. "Economics of Additive Manufacturing for End-Usable Metal Parts." *The International Journal of Advanced Manufacturing*. http://www.springerlink.com/index/K08M081535085168.pdf.

Barnard, Noel. 1961. "Bronze Casting and Bronze Alloys in Ancient China." http://www.bcin.ca/Interface/openbcin.cgi?submit=submit&Chinkey=63387.

Bassoli, Elena, Andrea Gatto, Luca Iuliano, and Maria Grazia Violante. 2007. "3D Printing Technique Applied to Rapid Casting." *Rapid Prototyping Journal* 13 (3): 148–55.

Baumers, Martin. 2012. "Economic Aspects of Additive Manufacturing: Benefits, Costs and Energy Consumption." © Martin Baumers. https://dspace.lboro.ac.uk/dspace-jspui/handle/2134/10768.

Baumers, Martin, Phill Dickens, Chris Tuck, and Richard Hague. 2016/1. "The Cost of Additive Manufacturing: Machine Productivity, Economies of Scale and Technology-Push." *Technological Forecasting and Social Change* 102: 193–201.

Cheah, C. M., C. K. Chua, C. W. Lee, C. Feng, and K. Totong. 2004. "Rapid Prototyping and Tooling Techniques: A Review of Applications for Rapid Investment Casting." *International Journal of Advanced Manufacturing Technology* 25 (3-4): 308–20.

Conner, Brett P., Guha P. Manogharan, Ashley N. Martof, Lauren M. Rodomsky, Caitlyn M. Rodomsky, Dakesha C. Jordan, and James W. Limperos. 2014. "Making Sense of 3-D Printing: Creating a Map of Additive Manufacturing Products and Services." *Additive Manufacturing* 1–4 (October): 64–76.

Deng, Chengyang, Jinwu Kang, Haolong Shangguan, Yongyi Hu, Tao Huang, and Zhiyong Liu. 2018. "Effects of Hollow Structures in Sand Mold Manufactured Using 3D Printing Technology." *Journal of Materials Processing Technology* 255 (May): 516–23.

Gullapalli, Ram A. 2016. *A Study of Mixed Manufacturing Methods in Sand Casting Using 3D Sand Printing and FDM Pattern-Making Based on Cost and Time*. Youngstown State University.

Hackney, Philip, and Richard Wooldridge. 2017. "Optimisation of Additive Manufactured Sand Printed Mould Material for Aluminium Castings." *Procedia Manufacturing* 11 (January): 457–65.

Hopkinson, N., and P. Dickens. 2003. "Analysis of Rapid Manufacturing—using Layer Manufacturing Processes for Production." *Proceedings of the Institution of Mechanical Engineers, Part C: Journal of Mechanical Engineering Science* 217 (1): 31–39.

Hull, Charles, Michael Feygin, Yehudah Baron, Roy Sanders, Emanuel Sachs, Allan Lightman, and Terry Wohlers. 1995. "Rapid Prototyping: Current Technology and Future Potential." *Rapid Prototyping Journal* 1 (1): 11–19.

Joshi, Durgesh, and Bhallamudi Ravi. 2010. “Quantifying the Shape Complexity of Cast Parts.” *Computer-Aided Design and Applications* 7 (5): 685–700.
Manogharan, Guha, Richard A. Wysk, and Ola L. A. Harrysson. 2016. “Additive Manufacturing–integrated Hybrid Manufacturing and Subtractive Processes: Economic Model and Analysis.” *International Journal of Computer Integrated Manufacturing* 29 (5): 473–88.
Martof, Ashley N., and Brett P. Conner. 2017. “Evaluating Business Models Enabling Point of Need Additive Manufacturing for Maintenance and Sustainment (Preprint).” Youngstown State University Youngstown United States. http://www.dtic.mil/docs/citations/AD1042402.
Mun, Jiwon, Byoung-Gwan Yun, Jaehyung Ju, and Byung-Moon Chang. 2015. “Indirect Additive Manufacturing Based Casting of a Periodic 3D Cellular Metal – Flow Simulation of Molten Aluminum Alloy.” *Journal of Manufacturing Processes* 17 (January): 28–40.
Psarra, Sophia, and Tadeusz Grajewski. 2001. “Describing Shape and Shape Complexity Using Local Properties.” In *Proceedings 3rd International Space Syntax Symposium*, 28–21. Citeseer.
Shangguan, Haolong, Jinwu Kang, Chengyang Deng, Yongyi Hu, and Tao Huang. 2017. “3D-Printed Shell-Truss Sand Mold for Aluminum Castings.” *Journal of Materials Processing Technology* 250 (December): 247–53.
Singh, Rupinder. 2010. “Three Dimensional Printing for Casting Applications: A State of Art Review and Future Perspectives.” In *Advanced Materials Research*, 83:342–49. Trans Tech Publ.
Snelling, Dean, Heather Blount, Charles Forman, Kelly Ramsburg, Andrew Wentzel, Christopher Williams, and Alan Druschitz. 2013. “The Effects of 3D Printed Molds on Metal Castings.” In *International Solid Freeform Fabrication Symposium*. pdfs.semanticscholar.org. https://pdfs.semanticscholar.org/9186/f3369a27b35e99b494f8e66f080b75233686.pdf.
Staff, Mcdp. 2016. “Modest Growth in Worldwide Casting Market.” *Metal Casting Design and Purchasing*, February.
Thomas, Douglas S., and Stanley W. Gilbert. 2014. “Costs and Cost Effectiveness of Additive Manufacturing.” National Institute of Standards and Technology. https://doi.org/10.6028/NIST.SP.1176.
Upadhyay, Meet, Tharmalingam Sivarupan, and Mohamed El Mansori. 2017. “3D Printing for Rapid Sand casting—A Review.” *Journal of Manufacturing Processes* 29 (October): 211–20.
USITC. 2005. “Foundry Statistics.pdf.”
USITC, 2005. Foundry Products: Competitive Conditions in the US Market. United States International Trade Commission, Washington, DC.
Walker, Jason, Evan Harris, Charles Lynagh, Andrea Beck, Rich Lonardo, Brian Vuksanovich, Jerry Thiel, Kirk Rogers, Brett Conner, and Eric MacDonald. 2018. “3D Printed Smart Molds for Sand Casting.” *International Journal of Metalcasting*, February. https://doi.org/10.1007/s40962-018-0211-x.
Walker, Jason M., Emily Bodamer, Alex Kleinfehn, Yuanyuan Luo, Matthew Becker, and David Dean. 2017. “Design and Mechanical Characterization of Solid and Highly Porous 3D Printed Poly(propylene Fumarate) Scaffolds.” *Progress in Additive Manufacturing* 2 (1): 99–108.
Watson, Andrew B. 2011. “Perimetric Complexity of Binary Digital Images: Notes on Calculation and Relation to Visual Complexity,” February. https://ntrs.nasa.gov/search.jsp?R=20110013429.

\